Molecules **2007**, *12*, 290-296

molecules

ISSN 1420-3049
http://www.mdpi.org

Full Paper

Modeling of Acetylene Pyrolysis under Steel Vacuum Carburizing Conditions in a Tubular Flow Reactor†

Rafi Ullah Khan*, Siegfried Bajohr, Frank Graf and Rainer Reimert

Engler-Bunte-Institut, Bereich Gas, Erdöl und Kohle, Engler Bunte Ring 1, Universität Karlsruhe, D-76131 Karlsruhe, Germany; E-mails: siegfried.bajohr@ciw.uni-karlsruhe.de, frank.graf@ciw.uni-karlsruhe.de, rainer.reimert@ciw.uni-karlsruhe.de

* Author to whom correspondence should be addressed. E-mail: rafi_ullah.khan@ciw.uni-karlsruhe.de

† Paper presented at ECSOC-10, 1-30 November 2006

Received: 20 February 2007; in revised form: 1 March 2007 / Accepted: 1 March 2007 / Published: 2 March 2007

Abstract: In the present work, the pyrolysis of acetylene was studied under steel vacuum carburizing conditions in a tubular flow reactor. The pyrolysis temperature ranged from 650 °C to 1050 °C. The partial pressure of acetylene in the feed mixture was 10 and 20 mbar, respectively, while the rest of the mixture consisted of nitrogen. The total pressure of the mixture was 1.6 bar. A kinetic mechanism which consists of seven species and nine reactions has been used in the commercial computational fluid dynamics (CFD) software Fluent. The species transport and reaction model of Fluent was used in the simulations. A comparison of simulated and experimental results is presented in this paper

Keywords: Acetylene; Pyrolysis; Modeling; Simulation; Carburizing

---

Introduction

Amongst the many applications of acetylene, low pressure carburizing of steel is an up and coming one. The pyrolysis of acetylene has been studied by many researchers under various conditions, depending upon the application being considered. Detailed kinetic mechanisms proposed in literature

may consist of hundreds of species and reactions. Typically, these investigations include shock tube pyrolysis of acetylene [1–12] and pyrolysis in flow systems [13–15]. The deposition of pyrolytic carbon from various hydrocarbons has also been described by some researchers [16–20]. Although the detailed kinetic mechanisms are considered to be more accurate and reliable, their use is mostly limited to ideal flow models. Use of such detailed kinetic mechanisms is not easy with transport models in CFD softwares with current computational hardware and algorithms. Nevertheless, CFD softwares normally implement Navier-Stokes equations and are used for modeling the flow field, even when the geometry is complex. Operational kinetic mechanisms or reduced versions of detailed mechanisms can be used with CFD softwares for modeling the reacting flow. Vacuum carburizing with acetylene involves the pyrolysis of acetylene under low pressure, which produces solid pyrolytic carbon and soot along with other hydrocarbon gases, making the flow field more complex. Diffusion of carbon into the surface of steel takes place, which is continued until the desired carbon content and case depth are achieved. In the present work, the pyrolysis of acetylene was studied under such conditions suitable for vacuum carburizing of steel.

Results and Discussion

The measured pyrolysis products include CH_4, C_2H_2, C_2H_4, C_4H_4, C_6H_6.. The amount of carbon $C_{(s)}$ in the form of soot was calculated from a carbon mass balance of the measured gas phase products. The product yields have been plotted as a function of temperature. The experimental results are compared with the simulation results of Fluent version 6.2. The amount of hydrogen was also calculated by a material balance and is also compared with the simulation results. The temperature varies along the reactor length. Figure 1 shows the temperature profiles in the reactor at three different controller temperatures values.

Figure 1. Temperature profiles at selected controller temperatures Tc.

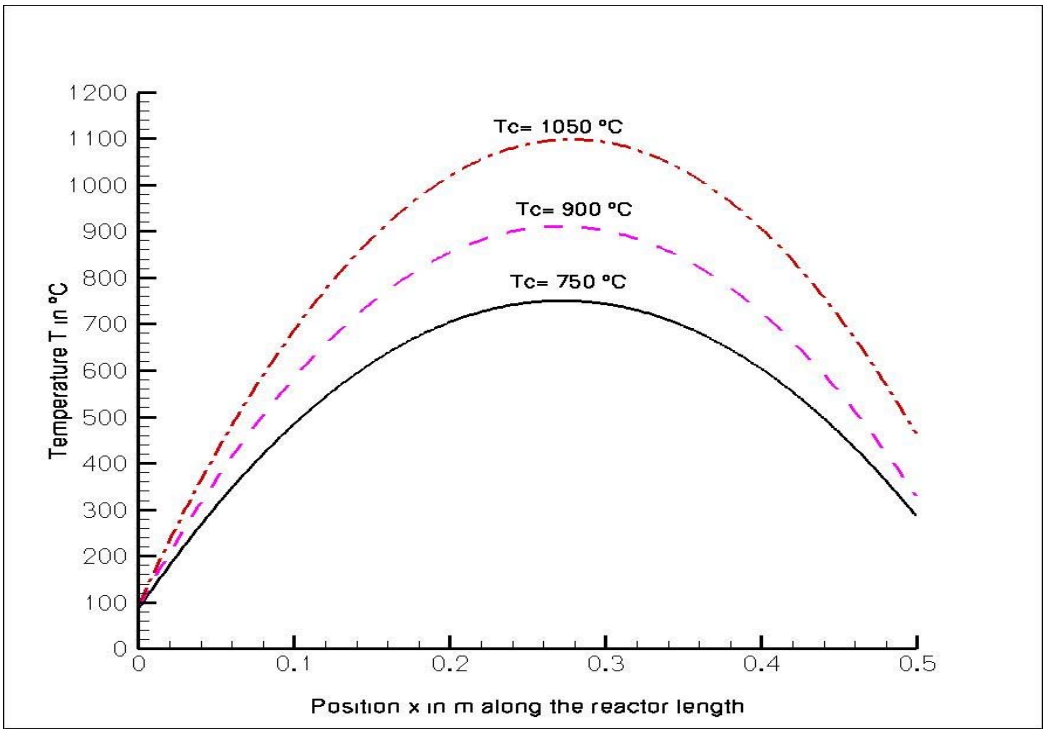

Figure 2. Mole fraction contours of C_2H_2 at 900 °C and 20 mbar partial pressure of acetylene.

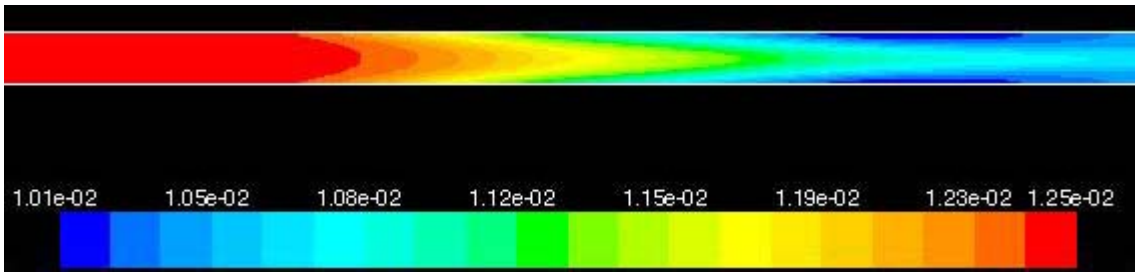

Figure 3. Mole fractions contours of $C_{(s)}$ at 900 °C and 20 mbar partial pressure of acetylene.

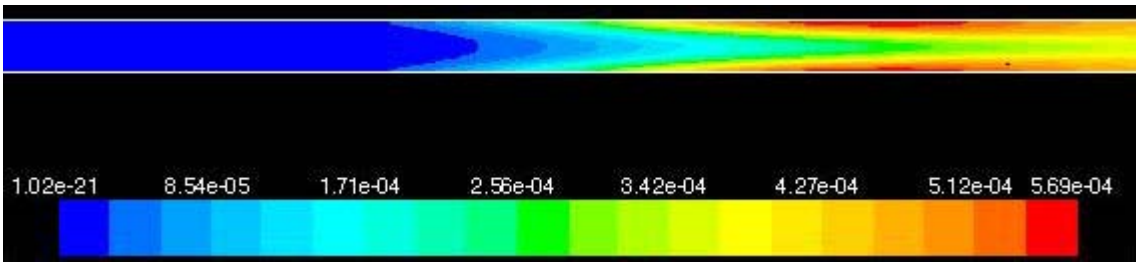

Figure 4. Comparison of simulated vs experimental results at 10 mbar acetylene partial pressure.

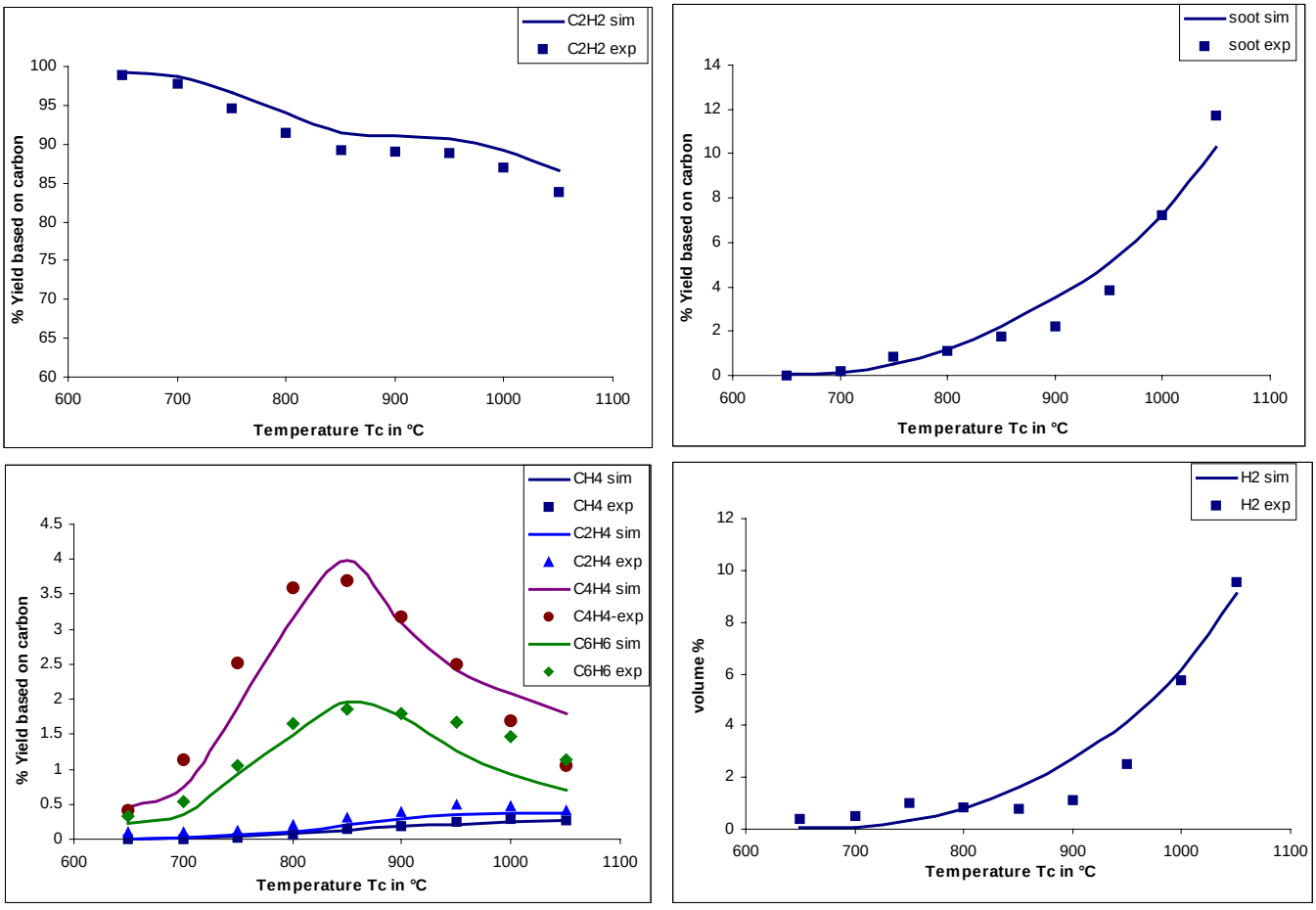

Figures 2 and 3 show two of the typical mole fraction contours obtained from simulations for the two important species C_2H_2 and C(s) at 900 °C and 20 mbar partial pressure of acetylene in the reactor. Figure 4 shows the comparison of experimental and simulation results for acetylene at 10 mbar partial pressure for a controller temperature variation of 650 °C to 1050 °C. The carbon content carried by unconverted acetylene in the mixture decreases from 99 % at 650 °C to 75 % at 1050 °C for 20 mbar, representing a 25 % conversion of acetylene to other products at the outlet, as shown in Figure 5. The second major and important component carrying carbon among the pyrolysis products is the soot, for which results are shown for 10 mbar as well as for 20 mbar partial pressure of acetylene. The percentage of carbon $C_{(s)}$ in the form of soot increases with an increase in temperature. The formation of C_4H_4 and C_6H_6 increases up to a temperature of 900 °C and then gradually decreases at higher temperatures. CH_4 and C_2H_4 are also formed, but the carbon content in these compounds is less than 1 % under these experimental conditions.

Figure 5. Comparison of simulated vs experimental results at 20 mbar acetylene partial pressure.

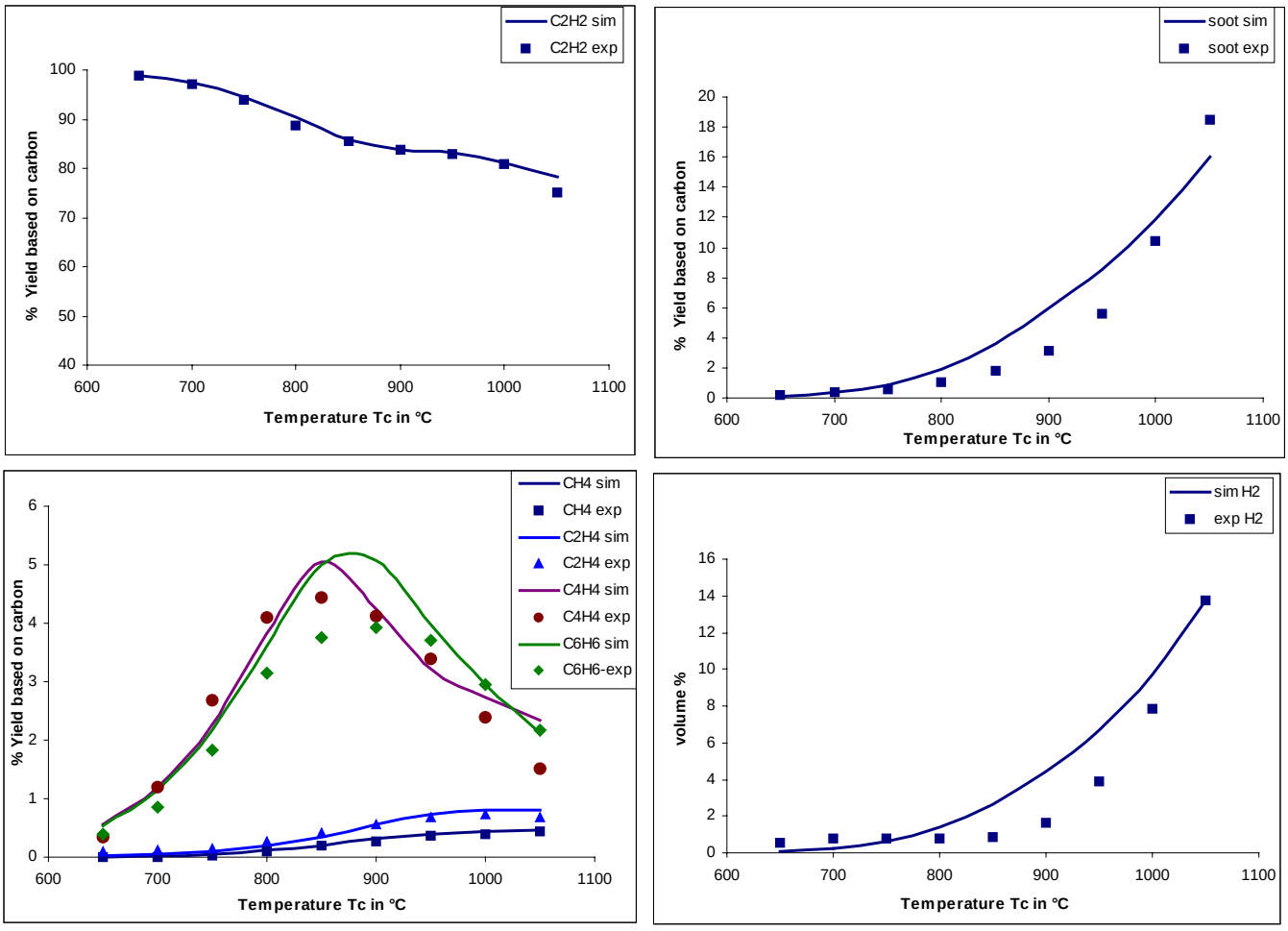

Reaction Mechanism and CFD Model

The reaction mechanism shown in Table 1 consists of seven species which are the major products of acetylene pyrolysis under vacuum steel carburizing conditions. These include $C_{(s)}$, which represents the solid carbon in the form of soot, and hydrocarbons, consisting of CH_4, C_2H_2, C_2H_4, C_4H_4, and C_6H_6, along with H_2. The overall mechanism consists of nine reactions. The estimated Arrhenius

parameters, activation energies and proposed reaction rates are also shown in Table 1. A 2-D grid consisting of 300 x 20 cells (6000 cells in total) has been used to represent a reactor length of 500 mm with a diameter of 20 mm. The species transport and reaction model in Fluent was used for modeling the chemistry. The mechanism discussed above was implemented through a user defined function (UDF) in Fluent. The operating pressure was set equal to 1.6 bar while inlet temperature and velocity boundary conditions were used according to the experimental measurements.

Table 1. Proposed reaction mechanism and kinetic parameters of acetylene pyrolysis.

Rate constant $k_i = A_i \cdot e^{\left(\frac{-E_{A,i}}{RT}\right)}$				
No.	**Reaction**	**Rate Expression**	**A_i (mol, m^3, sec)**	**$E_{A,i}$ (kJ/mol)**
1	$C_2H_2 + H_2 \rightarrow C_2H_4$	$r_1 = k_1 \cdot c_{C_2H_2} \cdot c_{H_2}^{0.36}$	$4.4 \cdot 10^3$	103.0
2	$C_2H_4 \rightarrow C_2H_4 + H_2$	$r_2 = k_2 \cdot c_{C_2H_4}^{0.5}$	$3.8 \cdot 10^7$	200.0
3	$C_2H_2 + 3H_2 \rightarrow 2CH_4$	$r_3 = k_3 \cdot c_{C_2H_2}^{0.35} \cdot c_{H_2}^{0.22}$	$1.4 \cdot 10^5$	150.0
4	$2CH_4 \rightarrow C_2H_2 + 3H_2$	$r_4 = k_4 \cdot c_{CH_4}^{0.21}$	$8.6 \cdot 10^6$	195.0
5	$C_2H_2 \rightarrow 2C_{(s)} + H_2$	$r_5 = k_5 \cdot \frac{c_{C_2H_2}^{1.9}}{1 + 18 c_{H_2}}$	$5.5 \cdot 10^6$	165.0
6	$C_2H_2 + C_2H_2 \rightarrow C_4H_4$	$r_6 = k_6 \cdot c_{C_2H_2}^{1.6}$	$1.2 \cdot 10^5$	120.7
7	$C_4H_4 \rightarrow C_2H_2 + C_2H_2$	$r_7 = k_7 \cdot c_{C_4H_4}^{0.75}$	$1.0 \cdot 10^{15}$	335.2
8	$C_4H_4 + C_2H_2 \rightarrow C_6H_6$	$r_8 = k_8 \cdot c_{C_2H_2}^{1.3} \cdot c_{C_4H_4}^{0.6}$	$1.8 \cdot 10^3$	64.5
9	$C_6H_6 \rightarrow 6C_{(s)} + 3H_2$	$r_9 = k_9 \cdot \frac{c_{C_6H_6}^{0.75}}{1 + 22 c_{H_2}}$	$1.0 \cdot 10^3$	75.0

As the reactor is not operated under isothermal conditions, a temperature profile was necessary to model the temperature field. A mathematical fit in the form of a polynomial shown in equation (1) below was used to describe the temperature profile in the simulations:

$$T(T_c, x) = (a \cdot x^2 + b \cdot x + c) \cdot T_c + d \cdot x^2 + e \cdot x + f \quad (1)$$

where $T(T_c,x)$ represents the temperature as a function of the controller temperature T_c and the position x along the reactor length, whereas a, b, c, d, e and f are the polynomial coefficients obtained by least squares fit to the experimental results. This temperature profile was also implemented through a user defined function (UDF) and compiled before loading into Fluent using the default procedures in the software. A typical temperature profile implemented in Fluent is shown in Figure 1. The solution was converged to species residuals of 10^{-6} or less so that there was no further variation of these residuals. The convergence was fast and achieved in less than 500 iterations.

Conclusions

Acetylene pyrolysis has been modeled by using simplified chemistry with a transport model under the particular conditions of the industrial process of vacuum carburizing of steel. Comparison of simulated and experimental results shows satisfactory agreement under technical operating conditions.

Further investigations for complex geometries are necessary to prove the validity of the model for the application as a prediction tool to control the carburizing process in commercial plants.

Experimental

A ceramic reactor with an inner diameter of 20 mm, outer diameter of 25 mm and a length of 600 mm was used in the present investigation. There is a ceramic filter at the outlet of the reactor which can separate entrained solid carbon from the gas stream. The pyrolysis products in the gas phase were measured by gas chromatography. The temperature profile was measured at the center of the reactor in an interior ceramic pipe with an outer diameter of 6 mm.

Acknowledgements

The financial assistance of the Higher Education Commission of Pakistan (HEC) and the German Academic Exchange Service (DAAD) are gratefullly acknowledged.

References

1. Wu, C. H.; Singh, H. J.; Kern, R. D. Pyrolysis of acetylene behind reflected shock waves. International. *Int. J. Chem. Kin.* **1987**, *19*, 975-996.
2. Frenklach, M.; Durgaprasad, M. B.; Taki, S.; Matula. R. Soot formation in shock-tube pyrolysis of acetylene, allene, and 1, 3-butadiene. *Combust. Flame* **1983,** *54*, 81-101.
3. Frenklach, M.; Clary, D. W.; Gardiner, W. C.; Stein. S. E. Detailed kinetic modeling of soot formation in shock-tube pyrolysis of acetylene. *Proc. Combust. Inst.* **1984**, *20*, 887-901.
4. Frenklach, M. Reaction mechanism of soot formation in flames. *Phys. Chem. Chem. Phys.* **2002**, *4*, 2028-2037.
5. Back, M. H. Mechanism of the Pyrolysis of Acetylene. *Can. J. Chem.* **1971**, *49*, 2199–2204.
6. Kiefer J. H.; Von Drasek, W. A. The mechanism of the homogeneous pyrolysis of acetylene. *Int. J. Chem. Kinet.* **1990**, *22*, 747-786.
7. Gay, I. D.; Kistiakowsky, G. B.; Michael, J. V.; Niki, H. Thermal decomposition of acetylene in shock waves. *J. Chem. Phys.* **1965**, *43*, 1720-1726.
8. Kruse, T.; Roth, P. Kinetics of C2 Reactions during High-Temperature Pyrolysis of Acetylene. *J. Phys. Chem. A.* **1997**, *101*, 2138–2146.
9. Tanzawa, T.; Gardiner, W. C., Jr. Reaction mechanism of the homogeneous thermal decomposition of acetylene. *J. Phys. Chem.*. **1980**, *84*, 236-239.
10. Laskin, A.; Wang, H. On initiation reactions of acetylene oxidation in shock tubes- A quantum mechanical and kinetic modeling study. *J. Chem. Phys. Lett.* **1999**, *303*, 43-49.
11. Kiefer, J. H.; Sidhu, S. S.; Kern, R. D.; Xie, K.; Chen, H.; Harding, L. B. The homogeneous pyrolysis of acetylene II: the high temperature radical chain mechanism. *J. Combust. Sci. Tech.*. **1992**, *82*, 101-130.
12. Böhm H.; Jander, H. PAH formation in acetylene-benzene pyrolysis. *Phys. Chem. Chem. Phys.* **1999**, *1*, 3775-3781.

13. Norinaga, K.; Deutschmann, O.; Hüttinger, K. J. Analysis of gas phase compounds in chemical vapor deposition of carbon from light hydrocarbons. *Carbon* **2006**, *44*, 1790-1800.
14. Dimitrijevic, S. T.; Paterson, S.; Pacey. P. D. Pyrolysis of acetylene during viscous flow at low conversions; influence of acetone. *J. Anal. App. Pyrol.* **2000**, *53*, 107-122.
15. Cullis, C. F.; Franklin, N. H. The pyrolysis of mixtures of acetylene with other hydrocarbons. *J. Combust. Flame* **1964**, *8*, 246-248.
16. Krestinin, A. V. On the Kinetics of Heterogeneous Acetylene Pyrolysis. *Kinet. Catal.* **2000**, *41*, 729-736.
17. Hu, Z. J.; Hüttinger, K. J. Mechanisms of carbon deposition-A kinetic approach. *Carbon* **2002**, *40*, 624-628.
18. Hu, Z. J.; Hüttinger, K. J. Influence of the surface area/volume ratio on the chemistry of carbon deposition from methane. *Carbon* **2003**, *41*, 501-1508.
19. Norinaga, K.; Hüttinger, K. J. Kinetics of surface reactions in carbon deposition from light hydrocarbons. *Carbon* **2003**, *41*, 1509-1514.
20. Zhang, W. G.; Hu, Z. J.; Hüttinger, K. J. Chemical vapor infiltration of carbon fiber felt: optimization of densification and carbon microstructure. *Carbon* **2002**, *40*, 2529-2545.